Published in final edited form as:

Inorg Chem. 2011 July 4; 50(13): 6210–6219. doi:10.1021/ic200491z.

Design and Synthesis of a Bombesin Peptide-Conjugated Tripodal Phosphino Dithioether Ligand Topology for the Stabilization of the *fac*-$[M(CO)_3]^+$ Core (M = ^{99m}Tc or Re)

Raghuraman Kannan[*,†], **Nagavarakishore Pillarsetty**[†], **Hariprasad Gali**[†], **Timothy J. Hoffman**[‡,||], **Charles L. Barnes**[§], **Silvia S. Jurisson**[§], **Charles J. Smith**[†,||], and **Wynn A. Volkert**[†]

[†]Department of Radiology, University of Missouri, Columbia, Missouri 65211

[‡]Department of Internal Medicine, University of Missouri, Columbia, Missouri 65211

[§]Department of Chemistry, University of Missouri, Columbia, Missouri 65211

[||]H. S. Truman Memorial VA Hospital, University of Missouri, Columbia, Missouri 65211

Abstract

A new tumor-seeking tridentate topology consisting of a phosphino dithioether ($(HOCH_2)_2PCH_2CH_2S(CH_2)_nCH_2SR$; PS_2) ligand framework for the production of kinetically inert and *in vivo* stable facial $[^{99m}Tc(CO)_3(PS_2)]^+$ or $[Re(CO)_3(PS_2)]^+$ is described. The X-ray crystal structure of *fac*-$Re(CO)_3(PS_2)PF_6$ is reported. The bioconjugation strategies for incorporating bombesin (BBN) peptides on to the PS_2 tripodal framework and, thereby, de novo designing of GRP receptor-seeking $Tc(PS_2–BBN)(CO)_3$ are developed.

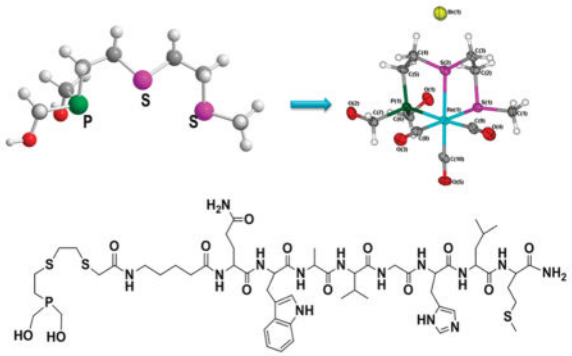

INTRODUCTION

Advances in metal-based molecular imaging and therapy agents will hinge upon discoveries in ligand architecture and coordination chemistry of specific transitionmetals.[1] For example,

*Corresponding Author: kannanr@health.missouri.edu.

Supporting Information. ^{13}C NMR data and NMR spectra. This material is available free of charge via the Internet at http://pubs.acs.org.

phosphine-based ligating frameworks have been shown to impart *in vivo* stability to radioactive metals through chelate interactions, and such agents have been utilized for biomedical applications.[2] It is very well established that the steric and electronic properties of phosphines exert a major influence on bonding interactions with transition metals of biological interest, thus, creating a compelling scenario for the *de novo* design of new functionalized phosphines.[3] Specifically, water-soluble phosphines functionalized with peptides or other biomolecules serve as biological markers for the *in vivo* targeting of receptors overexpressed in tumors for diagnostic/therapeutic use.[3] Surprisingly, despite the importance of peptide–phosphine conjugates in biomedical applications, little effort has been directed toward developing the synthetic strategies for the immobilization of biomolecules on water-soluble phosphine ligands.

Technetium-99m occupies a special position in inorganic radiopharmaceuticals[1,4,5] because of the following reasons: (i) optimal nuclear properties ($t_{1/2}$ = 6.02 h, $E(\gamma)$ =140 keV) for molecular imaging; (ii) easy availability through the transportable $^{99}Mo/^{99m}Tc$ generator system; and (iii) conversion to clinically useful, ligand exchangeable inorganic complexes for biomolecule conjugation. More importantly, ^{99m}Tc has a versatile inorganic chemistry, spanning different oxidation states, to produce a variety of ligand exchangeable coordination complexes.[1] Among several precursor complexes of technetium, the kinetically inert $[^{99m}Tc(CO)_3(H_2O)_3]^+$ complex has attracted much attention in recent years due to its commercial availability as the *Isolink* kit and ease of generation under clinical settings.[5] In fact, three water molecules in the complex can be replaced by a chelating ligand conjugated to a biomolecule such as a tridentate ligand or a “2+1” mixed ligand system, to yield a stable complex for targeted *in vivo* imaging applications. Alberto and co-workers have examined a library of N and S donor ligands for stabilizing the *fac*-$[M\text{-}(CO)_3]^+$ moiety.[6] Their investigations showed that by judicious selection of the ligand system, effective labeling of biomolecules could be achieved.[7] Likewise, Smith and co-workers have shown that the combination of bidentate N-donor ligands with a water-soluble monophosphine was effective in stabilizing the tricarbonyl core.[8] On the inorganic chemistry front, novel tridentate N-donor ligand systems were developed by Marzilli and coworkers for the effective stabilization of the $M(CO)_3$ moiety. They have shown that organic soluble metal precursors can serve as *synthons* for effective radiolabeling.[9] In addition, electron-rich bidentate O-donor ligands (*β*-diketones acetylacetone and curcumin) along with monodentate nitrogen ligands have been explored to generate stable *fac*-$[M(CO)_3(OO)(N)]^+$ complexes. [10] However, precise knowledge of ligand design is not completely understood—more specifically, which combinations of hard bases vs soft donors would lead to enhanced *in vivo* stability of the $[^{99m}Tc(CO)_3]^+$ moiety in order to engineer the design and development of organ-specific (or tumor-specific) radiopharmaceuticals.

In this respect, as part of our ongoing drug discovery program,[11] we have investigated pharmacophore motifs of a library of ligands encompassing hard nitrogen donors, phosphine π acids, and sulfur-containing soft donors. We, herein, report the development of ligand frameworks spanning the tripodal coordination sites of $[^{99m}Tc(CO)_3(H_2O)_3]^+$. The results reported herein encompass our successful chemistry for the synthesis of the phosphino dithioether ($(HOCH_2)_2PCH_2CH_2S(CH_2)_nCH_2\text{-}SCH_3$; PS_2) tripodal ligand backbone, its

conjugation with bombesin peptide, and the "proof of principle" that such a π-acid phosphine (P) and soft σ-donor thioether (S) topology will produce *in vivo* stable imaging agents. As a first step toward establishing the utility of the PS_2 ligand framework for *in vivo* biomedical applications, we focused our efforts on the synthesis of bifunctional ligand systems, bioconjugation with receptor-avid bombesin peptide, complexation with ^{99m}Tc and Re carbonyl complexes, and *in vivo* stability studies in mice.

Bombesin (BBN), a 14-amino-acid peptide, was first isolated from the skin of the frog amphibian *Bombina*.[12] BBN functions as a potent autocrine or paracrine growth factor for cells.[13] In the past decade, a plethora of information has been generated on BBN/receptor expression and physiological processes.[14] BBN shows high affinity for the gastrin-releasing peptide (GRP) receptor subtype BB2.[14] GRP receptors are overexpressed in many cancers, including prostate, breast, and small cell lung cancer.[15] Analogues of bombesin with modified structures have exhibited a similar or even higher affinity for these receptors. Synthetic peptides can be readily generated through automated solid phase techniques. For our studies, we have synthesized and utilized the seven-amino-acid truncated bombesin analogue (BBN) as a vehicle to target GRP receptors. The results reported in this paper include (i) synthesis and characterization of PS_2 ligand systems, (ii) synthesis and X-ray crystallographic investigation of the $[Re(CO)_3(PS_2)]^+$ complex, (iii) synthesis of the bifunctional PS_2 ligand system and bioconjugation with the truncated bombesin peptide, (iv) synthesis and *in vivo* stability analysis of $[^{99m}Tc(CO)_3(PS_2)]^+$ in mice, and (v) synthesis and *in vivo* stability analysis of $[^{99m}Tc(CO)_3(PS_2–BBN)]^+$ in mice.

RESULTS AND DISCUSSION

Synthesis of $(HOCH_2)_2PCH_2CH_2S(CH_2)_nCH_2SCH_3$ (n = 1 (4a), 2 (4b))

The synthesis of the PS_2 ligand system (**4a** and **4b**) was accomplished with a multistep synthetic route as shown in Scheme 1. In the first step, mono S-alkylation of 1,2-ethanedithiol or 1,3-ethane dithiol was achieved by treating diethyl-2-bromoethylphosphonate with a large excess of the corresponding dithiol. Subsequently, the reduction of phosphonate groups in monothioether monothiol phosphonates (**1a**, **1b**) using lithium aluminum hydride yielded monothioether monothiol phosphine (**2a**, **2b**) in quantitative yields. The thiol groups in these phosphines were S-alkylated by treating them with methyl iodide in the presence of sodium hydride to yield **3a** or **3b**. It is noteworthy to recognize the fact that under the reaction conditions employed, no P alkylation was observed. In the final step, the P–H bonds in **3a** and **3b** were formylated with aqueous formaldehyde in the presence of 5 N HCl to yield the corresponding phosphonium chloride salt $[(HOCH_2)_3PCH_2CH_2S(CH_2)_nCH_2SCH_3]Cl$. These salts are highly stable and can be stored in a refrigerator for extended periods of time. Before utilization of the phosphonium salt for the metalation reaction, the salts were treated *in situ* with triethylamine to generate the corresponding *bis*-hydroxymethyl phosphine derivative $(HOCH_2)_2PCH_2CH_2SCH_2CH_2$-$SCH_3$ (PS_2 **4a**, **4b**). All of the intermediate compounds and the final products were characterized using ^{1}H, ^{13}C, and ^{31}P NMR spectroscopy. Only the final products were analyzed using mass spectrometry, as the intermediates were highly malodorous.

Synthesis of $[M(CO)_3(PS_2)]^+$ (M = Re (5), ^{99m}Tc (6))

Our next step was to evaluate the role of an increase in chelate size of the PS_2 ligand systems with the *fac*-$[M(CO)_3]^+$ moiety. As a first step, we investigated the interactions of PS^2 (**4a**, **4b**) ligands with the $[Re(CO)_3Br_3]^{2-}$ core (Scheme 2). Typically, aqueous solutions of PS_2 (**4a**, **4b**) ligands were treated with $[NEt_4]_2[Re(CO)_3Br_3]$ species in the presence of triethylamine, and the complexation products were analyzed using traditional analytical measurements. In the case of PS_2 (**4a**), complex $[Re(CO)_3(PS_2)]Br$ (**5**) was formed as a singular chemical product (Scheme 2). The chemical constitution of $[Re(CO)_3(PS_2)]Br$ (**5**) was confirmed using NMR, IR, and single crystal X-ray diffraction techniques. In contrast, the reaction of **4b** with $[NEt_4]_2[Re(CO)_3Br_3]$ yielded multiple products as indicated by NMR and HPLC techniques; products were intractable even after several chromatographic purifications. It is important to note here that ligand **4a** contains an ethyl linker whereas **4b** contains a propyl linker between thioether groups. The formation of multiple products by ligand **4b** may be attributed to the flexible three carbon linker between the two sulfur atoms. This topology of three carbon atoms, presumably, initiates the formation of polymeric products, connecting to more than one rhenium atom.

Next, we investigated the interaction of PS_2 (**4a**) with the organometallic technetium tricarbonyl precursor $[^{99m}Tc(CO)_3\text{-}(OH_2)_3]^+$, and this reaction yielded the corresponding complex $[^{99m}Tc(CO)_3PS_2]^+$ (**6**) in near quantitative yield, as shown in Scheme 2. The formation of **6** was analyzed by reversed phase HPLC utilizing a radiometric (γ) detector. Gradient conditions are described in the Experimental Section, and complex **6** elutes with a retention time of 9.45 min, similar to rhenium analog **5**, which has a retention time of 9.5 min (determined using a UV detector). Figure 1 shows the comparative HPLC chromatogram of complexes **5** and **6**. The close lying retention times between complexes **5** and **6** further ascertain the structural similarity of these complexes. Also, we investigated the reaction of **4b** with a technetium carbonyl precursor. Similar to the reaction of **4b** with rhenium carbonyl, the reaction of **4b** with $[^{99m}Tc(CO)_3\text{-}(OH_2)_3]^+$ yielded multiple species, as indicated by HPLC analysis.

In summary, the shorter reaction time and the formation of a single species, even under dilute conditions, indicate the high kinetic propensity of PS_2 (**4a**) toward forming complexes with $M(CO)_3^+$ species. This property of **4a** is attributed to the symbiosis of both a perfect chelate size and a perfect match between soft thioether and hydroxymethyl phosphine donors to the soft $[M(CO)_3]^+$ core.

In order to understand the molecular features of **5**, single crystals were grown by slow evaporation of a methanolic solution of **5**, and a detailed X-ray crystallographic investigation was performed. An ORTEP presentation of complex **5** is shown in Figure 2. X-ray crystallographic data for complex **5** are presented in Table 1. The geometry around the central rhenium atom is slightly distorted octahedral, with the carbonyls arranged facially around the metal center. The three remaining positions in the octahedron are occupied by two sulfur atoms and one phosphorus atom in the PS_2 ligand.

In Vitro Stability Studies

Complex **5** was challenged with a large excess of cysteine or human serum albumin (HSA) to establish the *in vitro* stability characteristics. Cysteine is a typical model chosen for these particular studies, as a number of potential metal-chelating thiol functionalities are present *in vivo* (e.g., cysteine, serum proteins, and glutathione), and HSA is the major constituent in the blood, which is rich in various hetero-atom donors. The ^{31}P NMR spectroscopic data of aliquots of each sample were taken at different time intervals, and these studies indicated that complex **5** remained intact even after 6 months of incubation, demonstrating that the PS_2 core provides *in vitro* stability to the Re(I) complex.

The stability of complex $[^{99m}Tc(CO)_3PS_2]^+$ (**6**) under different pH conditions was investigated, and the stability was analyzed using HPLC (Table 2). We next investigated the *in vitro* stability of **6** by incubating the purified complex with a solution of 0.2 M cysteine, 0.2 M histidine, or 3×10^{-5} M HSA (thiol content 0.04 equiv/mol) at 37 °C at physiological pH for up to 24 h. No detectable decomposition of **6** was observed under these conditions, indicating the high *in vitro* stability.

The stability studies on **5** and **6** have further confirmed that complexes derived from the PS_2 ligand framework **4a** with two carbon linkers between sulfur atoms impart stability to the resulting technetium or rhenium complexes. Therefore, complex **6** bearing a ligand with tripodal architecture with two carbon linkers between the sulfur atoms was selected for performing detailed *in vivo* biodistribution studies in CF-1 mice.

In Vivo Biodistribution Studies of 6

Biodistribution studies on normal CF-1 mice were performed by intravenous administration of **6** followed by an analysis of radioactivity in various organs at various different time points. Results of this study as a function of percent injected dose (%ID) and the percent injected dose per unit mass (%ID/g) are given in Table 3. The data indicate rapid clearance of **6** from the blood, with only 0.59 ± 0.31%ID remaining in the whole blood after the 1 h post injection period. In addition, the data indicate that complex **6** clears through both the hepatobiliary and renal urinary pathways. However, the hydrophobic nature of **6** makes it preferentially excrete through the hepatobiliary pathway, with radioactivity of 52.41 ± 17.06 and 3.06 ± 1.37% of the injected dose in the large and small intestines, respectively, after the 4 h post injection period. Accordingly, the excretions through the renal pathway reach 37.43 ± 18.83% of the injected dose 4 h after injection. More importantly, there was no significant accumulation of radioactivity in the kidneys (0.32 ±0.05%ID 4 h post-injection). Thus, this study indicates that PS_2 ligand systems are effective in interacting with the $[^{99m}Tc(CO)_3]^+$ core to produce complexes that demonstrate kinetic inertness under both *in vitro* and *in vivo* conditions.

Synthesis of PS_2–BBN (10)

We have subsequently explored further organic chemistry in the PS_2 core toward bioconjugation with receptor-specific peptides. First, our efforts were focused on incorporating a “–COOH” functionality on the PS_2 ligand framework, as summarized in Scheme 3. The monothiolphosphine intermediate **2** was utilized as the starting material for

the synthesis of the carboxylate functionalized PS_2 system. PS_2–COOH (**8**) was synthesized in a two-step procedure. In the first step, compound **2** was S-alkylated with bromo-*t*-butyl acetate in the presence of NaHin THF, followed by deprotection of the *t*-butyl group by bubbling dry HCl to yield **8** in quanitative yields.

To demonstrate the utility of **8** in synthesizing receptor-avid peptide–phosphine conjugates, a bombesin 5-Ava-BBN[7–14] analogue, was chosen. The eight-amino-acid-containing bombesin analogue can be used as a vehicle to target GRP receptors, which are overexpressed on a variety of tumor tissues.[15] The conjugation of phosphine **8** to the BBN analog was successfully achieved by combinatorial solid phase peptide synthesis (SPPS) as well as employing 2-(1H-benzotriazole-1-yl)-1,1,3,3-tetramethyluronium hexafluorophosphate (HBTU) as the activating agent in the presence of triethylamine to yield the bombesin peptide conjugate **9**, as described in Scheme 4. The BBN analog was synthesized using automated-SPPS, cleaved from the resin, and coupling with **8** was achieved in solution. The crude product obtained was purified by reversed phase HPLC using a UV detector. The HPLC purified compound **9** was characterized by $^{31}P\{^{1}H\}$ NMR spectroscopy and mass spectrometry. The ^{31}P- $\{^{1}H\}$ NMR spectrum of compound **9** shows a singlet at $\delta = -143.9$ ppm, which confirmed the presence of a primary phosphine group. The Electrospray Ionization Mass Spectrum (ESI-MS) of conjugate **9** shows a peak at 1233.5 (calculated M^+, 1232.5) corresponding to the M^+H^+ peak and further establishing the identity of **9**. The phosphine–peptide conjugate **9** was converted into the corresponding hydroxymethyl phosphonium salt **10**, as shown in Scheme 4. The phosphonium salt **10** was purified by reversed phase HPLC to yield the pure product as a fluffy white powder. The ^{31}P NMR spectrum of **10** in water shows a sharp singlet at $\delta = 24.2$ ppm, which is typical for the tetrakis(hydroxymethyl) phosphonium group. Electrospray mass spectrometry of the product showed a peak at 1323.0 (*m*/*z*), further confirming the presence of the phosphonium salt **10**.

Synthesis and *in Vitro* Stability of $[^{99m}Tc(CO_3)PS_2–BBN]^+$(11)

The $[^{99m}Tc(CO)_3]^+$ complex of PS_2-5-Ava-BBN- [7–14]NH_2 (PS_2 –BBN) (**11**) was synthesized by incubation of PS_2–BBN (**10**) with $[^{99m}Tc(CO)_3(OH_2)_3]^+$ at pH 7.5–8.0 for 30 min at room temperature (25 °C) to yield the corresponding complex $[^{99m}Tc(CO)_3(PS_2 – BBN)]^+$ (**11**) in greater than 95% yields, as determined via radiometric detection on HPLC analysis. *In vitro* stability of complex **11** was studied by incubating the HPLC purified complex with a solution of 0.2 M cysteine, 0.2 Mhistidine, or 2% HSA solution in saline at pH 7.4 at 37 °C, and the radiochemical purity of the complex at different time points was analyzed by HPLC. The study indicated no detectable decomposition even at 24 h post-incubation.

In Vivo Biodistribution Studies of 11

In vivo biodistribution studies were performed in normal CF-1 mice by intravenous administration of the $[^{99m}Tc(CO)_3PS_2–BBN]^+$ (**11**) complex. Results of this study as a function of the percent injected dose (%ID) and the percent injected dose per unit mass (%ID/g) are given in Table 4. The $[^{99m}Tc(CO)_3PS_2–BBN]^+$ complex showed rapid clearance from the blood pool with activities reaching 1.9 ± 2.5% injected dose within 1 h post-injection and 0.43 ± 0.12% injected dose within 4 h post-injection. In addition, data on

the accumulation of radioactivity in blood (0.67% ID at 1 h and 0.0% ID at 24 h) and the stomach (0.93% ID/g at 1 h and 1.11% ID/g at 24 h) provide pharmacokinetic evidence for the *in vivo* stability of **11**. $[^{99m}Tc(CO)_3PS_2–BBN]^+$ (**11**) exhibited renal clearance with radioactivity reaching 0.49 ± 0.03% injected dose within 1 h post-injection. The amount of radioactivity found in the stomach, an indication of *in vivo* decomposition of a ^{99m}Tc conjugate, was negligible at 1 h (0.52 ± 0.22%ID) and 24 h (0.84 ± 0.67%ID) post-injection. There was retention of the conjugate in the liver (3.30 ± 0.74% ID, 4 h PI). The retention in the liver is due to the high hydrophobic nature of conjugate **11**.

The results provide important evidence that the PS_2–BBN ligand is able to produce *in vivo* stable complexes with $[^{99m}Tc(CO)_3(OH_2)_3]^+$. An uptake of radioactivity was observed in the pancreas with activity reaching 3.06 ± 1.08% ID (8.69 ± 2.07%ID/g) 1 h post-injection, as compared to $[^{99m}Tc(CO)_3\text{- }PS_2]^+$ complex **6**, which had very limited uptake in the pancreas (0.37 ± 0.18% injected dose (1.13 ± 0.48% ID/g) 1 h post-injection (Figure 3)). This result demonstrates the ability of the $[^{99m}Tc(CO)_3PS_2–BBN]^+$ complex to target GRP-receptor expressing cells *in vivo*. Acini cells in the pancreas express GRP receptors that are accessible to the bloodstream, and hence complex **11** is able to target the pancreas. The pancreas to muscle and pancreas to blood ratios (based on %ID per gram) reached a maximum of 58 and 13, respectively, at 1 h post-injection. The uptake of complex **11** in the pancreas is lower than values previously reported. For example, $^{99m}Tc(H_2O)(CO)_3$-Dpr-(SSS)-BBN[7–14]NH_2 showed an uptake of 23.3%ID/g and 10.2%ID/g in the pancreas and intestines, respectively, 1 h post-injection. [8a] In a similar fashion, our previous investigations utilizing BBN conjugated N-donor ligands labeled with $^{99m}Tc\text{- }(CO)_3{}^+$ have shown increased GRP receptor recognition under *in vivo* conditions.[8] In the present study, a five carbon spacer (5-aminovaleric acid) was used between the radioisotope and bombesin peptide, and it is possible that the closer proximity of the radionuclide and binding region may be one of the reasons for decreased uptake in the GRP receptor-avid pancreas. However, it is very well accepted that the spacer length between the radionuclide and binding region plays a key role in determining the *in vivo* affinity.[8] Our future studies will focus on two important aspects: (i) modulating the spacer length between the ligand and biomolecule and (ii) establishing that the accumulation of conjugate **11** is receptor-mediated by blocking with free peptides. The results presented in the paper establish that the "PS_2" ligand system is novel and effective in stabilizing the $[M(CO)_3]$ core under *in vitro* and *in vivo* conditions.

CONCLUSION

Among a library of hard nitrogen base donors, π-acid phosphine, and soft sulfur donor ligands screened so far, the kinetic inertness and thermodynamic stability displayed by "*facially*" spanning tridentate phosphinodithio ether (PS_2)-stabilized $[Tc(CO)_3(PS_2)]^+$/ $[Re(CO)_3(PS_2)]^+$ complexes is an intriguing discovery. Indeed, several previous reports involving facially spanning 1,4,7-trithia cyclononane ($9S_3$) complexes $[M(9S_3)_2]^+$ (M = Tc, Re, Ru, Os) provide evidence for the susceptibility of these systems for ethene loss.[16] While the incorporation of a phosphine center within the macrocyclic framework (e.g., $9PS_2$ ligands) improved the kinetic inertness of $[Mo(9PS_2)(CO)_3]^+$ in comparison with $[Mo(9S_3)(CO)_3]^+$, the reverse has been found to be true in a comparative study of $[Fe(9S_3)_2]^{2+}$ and

$[Fe(9PS_2)_2]^{2+}$.[16] In this context, results from our current studies have demonstrated that the compact PS_2 ligand system possesses topology for facial tridentate coordination with $Tc(CO)_3^+$/$Re(CO)_3^+$ cores, thereby producing five-membered $[M(CO)_3(PS_2)]^+$ (M = Tc/Re) compounds that are both kinetically robust and *in vivo* stable.

The aforementioned results presented herein demonstrate an effective and practically useful chemical basis for the stabilization of $[Tc(CO)_3]$/$[Re(CO)_3]^+$ cores and also for further conjugations of biologically useful metalated cores with tumor seeking peptides. Indeed, the results reported herein have wider implications in the areas of diagnostic and therapeutic biomedicine. The new approach of conjugating transition metals to biomolecules provides a straightforward route to the design and development of cancer diagnostic agents. Additionally, the incorporation of phosphines onto peptides (and proteins) will also help to engineer metal binding sites, which may eventually provide conformational integrity, biospecificity, and enhanced enzymatic activities. The combination of the dithioether with a phosphine moiety is unprecedented in technetium carbonyl chemistry. The *in vivo* stability of technetium complexes **6** and **11** imparted by the tripodal framework **4a** has provided a new pharmacophore to deliver the diagnostic or the therapeutic dose at the tumor site for potential applications in the care and treatment of cancer patients.

EXPERIMENTAL SECTION

All reactions were carried out under nitrogen with standard Schlenk techniques. All chemicals were obtained from Aldrich Chemical Co. and were used without further purification. NMR spectra were recorded on a Bruker ARX-300 spectrometer using the specified solvent; ^1H and ^{13}C chemical shifts are reported in ppm, downfield from internal standard $SiMe_4$, $^{31}PNMR$(121.5 MHz) with 85%H_3PO_4 as an external standard, and positive chemical shifts downfield of the standard. Combustion analysis was done by Oneida Research Services, Whitesboro, New York.

Synthesis of $(EtO)_2P(O)CH_2CH_2S(CH_2)_nCH_2SH$ (1a, 1b)

To an ice cold (0 °C) solution of 1,2-ethanedithiol (2.80 mL, 33.38 mmol) in THF (5 mL) was added dropwise a 60% suspension of sodium hydride (0.212 g, 5.305 mmol) in THF, and the resulting solution was stirred for 10 min. Bromoethyldiethylphosphonate (1.00 g, 4.08 mmol) was added dropwise, and the stirring was continued for 2 h. Excess sodium hydride was quenched by the addition of 4 mL of water. The solution was extracted into ethylacetate (3 × 20 mL), and the organic layer was dried over anhydrous sodium sulfate. Solvent was removed *in vacuo* to afford $(EtO)_2P(O)CH_2CH_2SCH_2CH_2SH$ (**1a**) in 96% yield (1.02 g). ^1HNMR ($CDCl_3$, 300 MHz): δ 4.11 (m, 4H, $P(O)CH_2CH_3$), 2.78 (m, 6H, SCH_2), 2.03 (m, 2H, PCH_2), 1.72 (t, 1H, SH), 1.33 (t, 6H, $P(O)CH_2CH_3$). $^{13}C\{^1H\}$ NMR ($CDCl_3$, 75 MHz): δ 61.70 (d, $P(O)CH_2CH_3$), 35.94 (s, SCH_2CH_2S), 26.71 (d, J_{P-C} = 136.80 Hz, P-CH_2), 24.71 (d, $^2J_{P-C}$ = 3.69 Hz, PCH_2CH_2S), 24.34 (S, CH_2), 16.32 (d, $P(O)CH_2CH_3$). $^{31}P\{^1H\}$NMR ($CDCl_3$, 121 MHz): δ 25.30 (s).

Synthesis of $H_2PCH_2CH_2SCH_2CH_2SH$ (2)

To a stirring solution of $(EtO)_2P(O)CH_2CH_2SCH_2CH_2SH$ (**1**; 0.95 g, 3.6 mmol) in anhydrous diethyl ether (15 mL) was added dropwise a 1 M solution of lithium aluminum hydride (4.7 mL, 4.7 mmol) in diethyl ether, and the stirring continued for 60 min. Excess lithium aluminum hydride was destroyed by the careful addition of wet ether, and finally 4 mL of 5 N HCl was added to dissolve the precipitate. The organic layer was diluted with diethyl ether (50 mL), washed with brine (2 × 30 mL), and dried using anhydrous sodium sulfate. Solvent was removed under reduced pressure to afford pure product $H_2PCH_2CH_2SCH_2CH_2SH$ (**2**) in 90% yield (492 mg). ^{1}H NMR ($CDCl_3$, 300 MHz): δ 2.77 (dt, 2H, PH_2, $^1J_{P–H}$ = 196.50 Hz, $^3J_{H–H}$ = 9.00 Hz), 2.73 (m, 6H, SCH_2), 1.73–1.80 (m, 2H, P-CH_2). ^{13}C{^{1}H}NMR ($CDCl_3$, 75 MHz): δ 35.84 (s, SCH_2), 34.97 (s, CH_2), 24.61 (s, $HSCH_2$), 14.83 (d, $J_{P–C}$ = 11. 45 Hz, P-CH_2). ^{31}P {^{1}H} NMR ($CDCl_3$, 121 MHz): δ −140.65 (s).

Synthesis of $H_2PCH_2CH_2SCH_2CH_2SCH_3$ (3)

To a suspension of sodium hydride (115 mg, 4.8 mmol) in anhydrous THF (3 mL) was added dropwise a solution of $H_2PCH_2CH_2SCH_2CH_2SH$ (**2**; 570.5 mg, 3.7 mmol) in THF (5 mL), and it was stirred for 20 min. To this suspension, methyl iodide (0.5 mL, 7.3 mmol) was added and stirred for 2 h. Excess sodium hydride was destroyed by slow addition of water (4 mL). The compound was extracted into ethyl acetate (3 × 20 mL), and the organic layer was dried using anhydrous sodium sulfate. Solvent was removed under reduced pressure to afford the pure product PS_2H_2 (**3**) in 60% yield (369 mg). ^{1}H NMR ($CDCl_3$, 300 MHz): δ 2.85 (dt, 2H, PH_2, $^1J_{P–H}$ = 196.83 Hz, $^3J_{H–H}$ = 6.07 Hz), 2.74 (m, 6H, SCH_2), 2.14 (s, 3H, SCH_3) 1.79 (m, 2H, P-CH_2). ^{13}C {^{1}H} NMR ($CDCl_3$, 75 MHz): δ 35.14 (s, SCH_2), 34.03 (s, CH_2), 31.34(s, SCH_2), 15.40 (s, SCH_3), 14.77 (d, $J_{P–C}$ = 11.20 Hz, P-CH_2). ^{31}P{^{1}H} NMR ($CDCl_3$, 121 MHz): δ −141.13 (s).

Synthesis of $Cl(HOCH_2)_3PCH_2CH_2SCH_2CH_2SCH_3$ (4a)

To a vigorously stirring suspension of $H_2PCH_2CH_2SCH_2CH_2SCH_3$ (**3**) (0.35 g, 2.10 mmol) in degassed ethanol (3 mL) was added a 37% w/w aqueous solution of formaldehyde (0.14 g, 4.90 mmol) and 2 N HCl (0.2 mL). The stirring was continued for 1 h and solvent removed under vacuum conditions to yield $Cl(HOCH_2)_3PCH_2CH_2SCH_2CH_2SCH_3$ (**4a**) in 80% yield (0.50 g). ^{1}H NMR (D_2O, 300 MHz): δ 4.76 (s, 6H, PCH_2O), 2.87–2.76 (m, 8H, CH_2), 2.09 (s, 3H, S-CH_3). ^{13}C {^{1}H} NMR (D_2O, 75 MHz): δ 50.21 (d, $J_{P–C}$ = 53.74 Hz, P-CH_2), 32.58 (s, SCH_2), 30.25 (s,CH_2), 22.74 (d, $J_{P–C}$ = 5.24 Hz, SCH_2CH_2P), 14.87 (d, $J_{P–C}$ = 38.19 Hz, SCH_2CH_2P), 13.85 (s, SCH_3). ^{31}P{^{1}H} NMR (D_2O, 121 MHz): δ 24.69 (s).

Synthesis of $(HOCH_2)_2PCH_2CH_2SCH_2CH_2SCH_3$ (4b)

Triethyl amine (20.2 mg, 0.20 mmol) was added to a vigorously stirring solution of **4a** (20 mg, 0.07 mmol) in degassed water (0.5 mL), and the resulting solution was stirred for 30 min. Solvent and excess triethylamine were removed in vacuo to obtain the crude product as a viscous oil. The crude product was purified on a C-18 reversed phase SepPak column, by elution with methanol–water (1:99) to obtain 13.5 mg of pure product **4b** (85% yield) as a clear viscous oil. (M^+H^+) calcd., 229.0486; obsd., 229.0482. ^{1}H NMR (D_2O, 300 MHz): δ

3.92 (t, 4H, J_{P-H} = 6 Hz, PCH_2O), 2.74–2.66 (m, 6H, CH_2), 2.00 (s, 3H, S-CH_3), 1.77 (bm, 2H, PCH_2CH_2). ^{31}P {^1H} NMR (D_2O, 121 MHz): δ −29.32 (s).

Synthesis of $[Re(CO)_3\{(CH_2OH)_2PCH_2CH_2SCH_2CH_2SCH_3\}]Br$ (5)

$[NEt_4][ReBr_3(CO)_3]$ (84 mg, 0.109 mmol) was dissolved in distilled water (1.5 mL), and the solution was stirred for 5 min to quantitatively generate $[Re(OH_2)_3(CO)_3]Br$. To this solution was added a solution of PS_2 (**4**; 24.8 mg, 0.109 mmol)$_8$ in 4 mL of water and 20 μL of triethylamine, and the resulting solution was stirred for 3 h. The progress of the reaction was monitored by $_{31}P$ NMR spectroscopy, and after the consumption of phosphine was complete, stirring was stopped and the solvent was removed under reduced pressure. The remaining solid was washed thrice with diethyl ether (3 × 5 mL) and dried. The solid obtained was washed several times with dichloromethane (4 × 3 mL) to remove traces of tetraethylammonium bromide and triethylammonium hydrochloride. The solid obtained was dried under vacuum conditions and dissolved in methanol to obtain crystals suitable for the X-ray diffraction study. ESI-MS (*m*/*z*): [M^+ – Br] calcd., 498.9; obsd., 499. ^1H (D_2O, 300 MHz, δ): 4.23 (s, 4H), 3.47–3.04 (m, 6H), 3.94–4.09 (m, 1H), 1.67–1.52 (m, 2H). $^{31}P\{^1H\}$ (D_2O, 121 MHz, δ): 39.65. Analysis calculated for $C_{10}H_{17}S_2O_5BrPRe$: C, 22.22%; O, 3.56%. Found: 22.01%; 3.07%.

In Vitro Stability Studies of 5

In order to determine the *in vitro* stability of the rhenium S_2P–rhenium complex **5**, 1 mg of **5** was dissolved in saturated solutions of cysteine and human serum albumin (HSA) in water at 25 °C. Cysteine is a typical model chosen for these particular studies, as a number of potential metal-chelating thiol functionalities are present *in vivo* (e.g., serum proteins and glutathione), and HSA is a major constituent in the blood. ^{31}P NMR spectroscopic data for aliquots of each sample were taken at different time intervals. The studies indicate the complex was stable even after 6 months of incubation.

Synthesis of $[^{99m}Tc(CO)_3(PS_2)]^+$ (6)

Complex **6** was prepared by adding a 200 μL solution of $[^{99m}Tc(CO)_3(OH_2)_3]^+$ (0.2–0.5 GBq) in saline to a solution of 50 μL of **4b** (0.05 mg/mL = 1.6×10^{-4} M) and 100 μL of 1 M $NaHCO_3$. The resulting solution was vortexed for 15 s and incubated for 30 min at RT to give the complex in >99% yield. The effective concentration of the PS_2 ligand is 2.4×10^{-5} M. The mobile phase for the HPLC consisted of a gradient system with solvent A corresponding to water with 0.1% trifluoroacetic acid (TFA) and solvent B corresponding to acetonitrile with 0.1% TFA. The HPLC gradient started with 95% A/5% B followed by a linear gradient from 95% A/5% B to 20% A/80% B for 2–18 min. The gradient remained at 20% A/80% B for 6 min between 18 and 24 min. The flow rate was 1.5 mL/min and the chart speed 0.5 cm/min. The formation of the complex was analyzed by reversed phase HPLC utilizing a radiometric (γ) detector. The retention time for the complex was 9.45 min and corresponds to the rhenium complex, which has a retention time of 9.5 min.

pH Stability Studies of $[^{99m}Tc(CO)_3(PS_2)]^+$ (6)

The crude $[^{99m}Tc(CO)_3(PS_2)]^+$ was peak purified on HPLC by collecting the fraction corresponding only to the complex. The acetonitrile in the solvent was removed by bubbling nitrogen gas for 1 h. The pH of the above solution was adjusted to different pH's with either 0.1 M NaOH or 0.1M HCl. The percent radiochemical stability (% RCP) of the resulting complex was analyzed by HPLC at 1, 4 ,and 24 h post-complexation.

In Vitro Stability Studies of $[^{99m}Tc(CO)_3(PS_2)]^+$ (6)

The *in vitro* stability of complex $[^{99m}Tc(CO)_3(PS_2)]^+$ (**6**) was measured as a function of time. The complex obtained was peak purified on HPLC by collecting the fraction corresponding only to the complex. The acetonitrile in the solvent was removed by bubbling nitrogen gas for 1 h. The purified complex was incubated with 0.2 M cysteine, 0.2 M histidine, and 2% HSA solution in saline at pH 7.4, and the radiochemical purity of the complex at different time points was analyzed by HPLC. No detectable decomposition of the chelate was observed under these conditions, indicating the high *in vitro* stability of the technetium complex **6**.

In Vivo Stability Studies of $[^{99m}Tc(CO)_3(PS_2)]^+$ (6)

The complex obtained was peak purified on HPLC by collecting the fraction corresponding only to the complex. The acetonitrile in the solvent was removed by bubbling nitrogen gas for 1 h. The biodistribution studies of the complex $[^{99m}Tc(CO)_3(PS_2)]^+$ were determined by injecting the peak purified complex in 4–6-week-old normal CF-1 mice (Charles River Laboratories, Wilmington, MA). The mice were injected via tail vein with 80–100 μL of the complex in a pH7 phosphate buffered saline containing 55–80 kBq of complex $[^{99m}Tc(CO)_3(PS_2)]^+$. The animals were sacrificed 0.5, 1, 4, and 24 h post-injection. The tissues and organs were excised from animals (N = 5 per group), rinsed in saline, weighed, and counted in a NaI(Tl) well counter. Percent injected dose (%ID) and %ID/g were calculated. Between 0.7 and 1.0 mL of blood was withdrawn from the heart via a cardiac puncture immediately after sacrifice and counted. It was assumed that the whole blood constituted 6.5% of the total body weight.

Synthesis of $H_2PCH_2CH_2SCH_2CH_2SCH_2COO^tBu$ (7)

To a suspension of sodium hydride (19 mg, 0.8 mmol) in anhydrous THF (3 mL) was added **2** (100 mg, 0.65 mmol) very slowly, and it was stirred for 30 min. To this suspension, *t*-butylbromoacetate (128 mg, 0.65 mmol) in anhydrous THF (2 mL) was added dropwise and stirred for 4 h. Excess sodium hydride was destroyed by the slow addition of water (3–4 mL). The compound was extracted into diethyl ether (4 × 20 mL), and the organic layer was dried with sodium sulfate. Solvent was removed under vacuum conditions to yield the crude product. The crude reaction mixture was purified on a silica gel column by eluting the product with a 1% ethylacetate/hexane solvent combination to yield the pure product in 80% yield (172 mg). ^{1}H NMR ($CDCl_3$, 300 MHz): δ 3.08 (s, 2H, SCH_2CO), 2.67 (dt, 2H, PH_2, $^1J_{P-H}$ = 195.00 Hz, $^3J_{H-H}$ = 6.01 Hz), 2.78–2.63 (m, 6H, SCH_2), 1.72–1.70 (m, 2H, P-CH_2), 1.41 (s, 9H, CCH_3). $^{13}C\{^1H\}$NMR ($CDCl_3$, 75 MHz): δ 169.30 (s, *C*OO^tBu), 81.32

(S, COO*C*(CH3)3), 34.92 (s, SCH_2CO), 34.56 (s, SCH_2), 32.18 (s, SCH_2), 27.80 (s, SCH_2), 14.71 (d, J_{P-C} = 11.25 Hz, P-CH_2). $^{31}P\{^1H\}$ NMR ($CDCl_3$, 121 MHz): δ −140.92 (s).

Synthesis of $H_2PCH_2CH_2SCH_2CH_2SCH_2COOH$ (8)

Dry HCl gas, generated *in situ* by the dropwise addition of sulfuric acid to sodium chloride, was bubbled through a solution of $H_2PCH_2CH_2SCH_2CH_2$- SCH_2COO^tBu (**7**; 120 mg, 0.44 mmol) in anhydrous methylene chloride for 30 min. The solution was stirred for 3 h and the solvent removed under reduced pressure to quantitatively yield H_2PS_2COOH ($H_2PCH_2CH_2SCH_2CH_2SCH_2COOH$) (**8**; 93 mg, 0.43 mmol). ^1H NMR ($CDCl_3$, 300 MHz): δ 3.31 (s, 2H, SCH_2CO), 2.77 (dt, 2H, PH_2, $^1J_{P-H}$ = 195.00 Hz, $^3J_{H-H}$ = 9.01 Hz), 2.92–2.43 (m, 6H, SCH2), 1.89–1.41 (m, 2H, P-CH_2). $^{13}C\{^1H\}$ NMR ($CDCl_3$, 75 MHz): δ 175.62 (s, COOH), 35.06 (s, SCH_2CO), 32.45 (s, SCH_2), 31.14 (s, SCH_2), 27.84 (s, SCH_2), 14.71 (d, J_{P-C} = 11.25 Hz, P-CH_2). $^{31}P\{^1H\}$ NMR ($CDCl_3$, 121 MHz): δ −141.26 (s).

Synthesis of H_2PS_2-5-Ava-BBN[7–14]NH_2(H_2PS_2BBN) (9)

A solution of 5-Ava-BBN[7–14]NH_2 (mol.wt.: 1024.21; 12 mg; 12 μmol) in DMF (0.5 mL) was added to a reaction mixture containing H_2PS_2- COOH(**8**; 3.8 mg; 18 μmol), HBTU(mol. wt.: 379.25; 6.8 mg; 18 μmol), and triethylamine (30 μL) in DMF (0.5 mL). The reaction mixture was stirred for 30 min at room temperature. The resultant phosphine–BBN conjugate was purified by reversed-phase HPLC and analyzed by ^{31}P NMR spectroscopy and electrospray mass spectrometry. The pure product (5.6 mg; 4.6 μmol; % yield ~ 38%) was obtained as a white powder. ^{31}P NMR (D_2O, 121 MHz, δ): δ −143.9 (s). ESI-MS (*m*/*z*) calcd., 1232.5 (M+); found, 1233.5 ($M^+ + H^+$).

Synthesis of S_2P-5-Ava-BBN[7–14]NH_2(PS_2–BBN) (10)

To a solution of phosphine PH_2S_2-5-Ava-BBN[7–14]NH_2 (**9**; 5 mg, 4 μmol) in ethanol (500 μL) and DMF (500 μL) were added 5 N hydrochloric acid (30 μL) and 37% aqueous formaldehyde (30 μL). The reaction mixture was stirred at room temperature (25 °C) for 30 min. The resultant phosphine–BBN phosphonium salt conjugate S_2P-5-Ava- BBN[7–14]NH_2(PS_2 –BBN) (**10**) was purified by reversed-phase HPLC and analyzed by ^{31}P NMR spectroscopy and electrospray mass spectrometry. The pure product (~55%) was obtained as a white powder. ^{31}P NMR (D2O): δ 24.2 (s). ESI-MS (*m*/*z*) calcd., 1323.6 (M^+ − Cl); found, 1323.0.

Synthesis of $[^{99m}Tc(CO)_3(PS_2–BBN)]^+$ (11)

The Tc-99m complex was prepared by adding a 250 μL solution of $[^{99m}Tc(CO)_3(OH_2)_3]^+$ (0.3–0.9 GBq) in saline to a solution of 50μL of PS_2–BBN(0.26 mg/mL = 1.9×10^{-4} M) and 50 μL of 1 M $NaHCO_3$. The resulting solution was vortexed for 15 s and incubated for 30 min at RT to give the complex in >99% yield. The mobile phase for the HPLC consisted of a gradient system with solvent A corresponding to water with 0.1% trifluoroacetic acid (TFA) and solvent B corresponding to acetonitrile with 0.1% TFA. The HPLC gradient started with 95% A/5% B followed by a linear gradient from 95% A/5% B to 30% A/70% B for 2–25 min. The gradient changed from 30% A/70% B to 5% A/95% B over a 5 min period

between 25 and 30 min. The flow rate was 1.5 mL/min and the chart speed 0.5 cm/min. Retention time for the complex was 17.33 min.

pH Studies of $[^{99m}Tc(CO)_3(PS_2–BBN)]^+$ (11)

The complex obtained was peak purified on HPLC by collecting the fraction corresponding only to the complex. The acetonitrile in the solvent was removed under reduced pressure by applying a vacuum for 1 h. The pH of the above solution was adjusted to different pH's with either 0.1M NaOH or 0.1 M HCl. The percent radiochemical stability of the resulting complex was analyzed by HPLC at 1, 4, and 24 h post-complexation.

In Vitro Studies of $[^{99m}Tc(CO)_3(PS_2–BBN)]^+$ (11)

The *in vitro* stability of the complex $[^{99m}Tc(CO)_3(PS_2–BBN)]^+$ was measured as a function of time. The complex obtained was peak purified on HPLC by collecting the fraction corresponding only to the complex. The acetonitrile in the solvent was removed under reduced pressure by applying a vacuum for 1 h. The purified complex was incubated with 0.2 Mcysteine, 0.2 M histidine, or 2% HSA solution in saline at pH 7.4, and the radiochemical purity of the complex at 25 °C was analyzed at different time points using radiometric HPLC.

In Vivo Studies of $[^{99m}Tc(CO)_3(PS_2–BBN)]^+$ (11)

Animal studies were performed in accordance with protocols approved by the Institutional Animal Care and Use Committee. The biodistribution studies of the complex $[^{99m}Tc(CO)_3(PS_2–BBN)]^+$ were determined by injecting complex **11** in normal 4–6-week-old CF-1 female mice (Charles River Laboratories, Wilmington, MA). The mice were injected via tail vein with 80–100 μL of the complex in pH 7 phosphate buffered saline containing 55–80 kBq of complex $[^{99m}Tc(CO)_3(PS_2–BBN)]^+$. The animals were sacrificed at 1, 4, and 24 h post-injection. The tissues and organs were excised from the animals (N = 5 per group), rinsed with saline, weighed, and counted in a NaI(Tl) well counter. The percent injected dose (%ID) and %ID/g were calculated. Between 0.7 and 1.0 mL of blood was withdrawn from the heart via cardiac puncture immediately after sacrifice and counted. It was assumed that the whole blood constituted 6.5% of the total body weight.

Crystallographic Data Collection and Refinement of Structure for 5

A suitable crystal was chosen and mounted on a glass fiber with epoxy resin. The crystal data and refinement results are given in the Supporting Information. Data reduction and processing followed routine procedures. Structures were solved by direct methods and refined on F_o^2. Absorption corrections were done by semiempirical equivalents. Crystal structure data for **5**: triclinic, space group $P\bar{1}$, a = 6.5967(4), b = 8.9236(5), c = 14.1771(8) Å, α = 89.0590(10), β = 79.3080(10), γ = 87.8210(10)°, V = 819.43(8)Å^3, Z = 2, ρ_{calcd} = 2.344 Mg cm^{-3}, $2\theta_{max}$ = 54.2°, MoKα radiation (λ = 0.71073 Å), T = 173 K. A colorless crystal with dimensions 0.45 × 0.15 × 0.15 mm^3 was grown by slow evaporation of an aqueous solution of **5**. No. reflns = 5882 (3538 > 2σ(I)), refinement of F^2, R_1 = 0.0548, wR_2 = 0.1508, GOF = 1.068.

Supplementary Material

Refer to Web version on PubMed Central for supplementary material.

Acknowledgments

This work was supported by funds from the U.S. Department of Energy (DE-FG02-01ER63192), Department of Radiology and the University of Missouri Research Reactor.

References

1. (a) Heeg MJ, Jurisson S. Acc Chem Res. 1999; 32:1053–1060.(b) Liu S. Chem Soc Rev. 2004; 33:445–461. [PubMed: 15354226] (c) Tweedle MF. Acc Chem Res. 2009; 42:958–968. [PubMed: 19552403] (d) Katayev EA, Kolesnikov GV, Sessler JL. Chem Soc Rev. 2009; 38:1572–1586. [PubMed: 19587953]
2. (a) Katti KV, Gali H, Smith CJ, Berning DE. Acc Chem Res. 1999; 32:9–17.(b) Kannan R, Nagavarakishore P, Volkert WA, Barnes C, Jurisson S, Katti KV. J Am Chem Soc. 2002; 124:7276–7277. [PubMed: 12071729] (c) Kothari KK, Gali H, Prabhu KR, Pillarsetty N, Owen NK, Katti KV, Hoffman TJ, Volkert WA. Nucl Med Biol. 2002; 29:83–89. [PubMed: 11786279] (d) Gali H, Hoffman TJ, Sieckman GL, Owen NK, Katti KV, Volkert WA. Bioconjugate Chem. 2001; 12:354–363.(e) Pillarsetty N, Katti KK, Hoffman TJ, Volkert WA, Katti KK, Kamei H, Koide T. J Med Chem. 2003; 46:1130–1132. [PubMed: 12646023] (f) Deutsch E. Radiochim Acta. 1993; 63:195–7.
3. (a) Fernandes C, Correia JDG, Gano L, Santos I, Seifert S, Syhre R, Bergmann R, Spies H. Bioconjugate Chem. 2005; 16:660–668.(b) Schiller E, Seifert S, Tisato F, Refosco F, Kraus W, Spies H, Pietzsch HJ. Bioconjugate Chem. 2005; 16:634–643.(c) Karra SR, Schibli R, Gali H, Katti KV, Hoffman TJ, Higginbotham C, Sieckman GL, Volkert WA. Bioconjugate Chem. 1999; 10:254–260.(d) Pillasetty N, Kannan R, Barnes CL, Katti KV. J Am Chem Soc. 2005; 127:331–336. [PubMed: 15631483] (e) Kannan RK, Katti KK, Barbour LJ, Pillarsetty N, Barnes CL, Katti KV. J Am Chem Soc. 2003; 125:6955–6961. [PubMed: 12783548] (f) Prabhu KR, Pillarsetty N, Gali H, Katti KV. J Am Chem Soc. 2000; 122:1554–1555.(g) Gilbertson SR, Collibee SE, Agarkov A. J Am Chem Soc. 2000; 122:6522–6523.
4. (a) Kereiakes, JG. Biophysical aspects:medical use of technetium-99m. American Institute of Physics; Woodbury, NY: 1992. (b) Helm L. Coord Chem Rev. 2008; 252:2346–2361.(c) Zolle, I., editor. Technetium-99 Radiopharmaceuticals: Preparation and Quality Control in Nuclear Medicine. 1. Springer; New York, NY: 2006. International Atomic Energy Agency. Trends in radiopharmaceuticals (ISTR-2005). proceedings of an international symposium organized by the International Atomic Energy Agency; Vienna. November 14–18, 2005; Vienna, Austria: International Atomic Energy Agency; 2007. (e) Nicolini, M.; Mazzi, U. Technetium, Rhenium, And Other Metals in Chemistry and Nuclear Medicine, 6. SGEd.iali; Padova, Italy: 2002. (f) Schwochau, K. Technetium: Chemistry and Radiopharmaceutical Applications. Wiley-VCH; Weinheim, Germany: 2000.
5. (a) Xavier C, Giannini C, Dall'Angelo S, Gano L, Maiorana S, Alberto R, Santos I. J Biol Inorg Chem. 2008; 13:1335. [PubMed: 18777182] (b) Maria L, Paulo A, Santos IC, Santos I, Kurz P, Spingler B, Alberto R. J Am Chem Soc. 2006; 128:14590. [PubMed: 17090043] (c) Hafliger P, Agorastos N, Spingler B, Georgiev O, Viola G, Alberto R. Chembiochem. 2005; 6:414. [PubMed: 15651047] (d) Rattat D, Schubiger PA, Berke HG, Schmalle H, Alberto R. Cancer Biother Radiopharm. 2001; 16:339. [PubMed: 11603005] (e) Amann A, Decristoforo C, Ott I, Wenger M, Bader D, Alberto R, Putz G. Nucl Med Biol. 2001; 28:243. [PubMed: 11323233] (f) Schibli R, La Bella R, Alberto R, Garcia-Garayoa E, Ortner K, Abram U, Schubiger PA. Bioconjugate Chem. 2000; 11:345.(g) Pietzsch HJ, Gupta A, Reisgys M, Drews A, Seifert S, Syhre R, Spies H, Alberto R, Abram U, Schubiger PA, Johannsen B. Bioconjugate Chem. 2000; 11:414.(h) Waibel R, Alberto R, Willuda J, Finnern R, Schibli R, Stichelberger A, Egli A, Abram U, Mach JP, Pluckthun A, Schubiger PA. Nat Biotechnol. 1999; 17:897. [PubMed: 10471933]

6. (a) Alberto R. Eur J Nucl Med Mol Imaging. 2003; 30:1299. [PubMed: 12898204] (b) Alberto R, Ortner K, Wheatley N, Schibli R, Schubiger AP. J Am Chem Soc. 2001; 123:3135. [PubMed: 11457025] (c) Schibli R, La Bella R, Alberto R, Garcia-Garayoa E, Ortner K, Abram U, Schubiger PA. Bioconjugate Chem. 2000; 11:345.(d) Pietzsch HJ, Gupta A, Reisgys M, Drews A, Seifert S, Syhre R, Spies H, Alberto R, Abram U, Schubiger PA, Johannsen B. Bioconjugate Chem. 2000; 11:414.(e) Egli A, Alberto R, Tannahill L, Schibli R, Abram U, Schaffland A, Waibel R, Tourwe D, Jeannin L, Iterbeke K, Schubiger PA. J Nucl Med. 1999; 40:1913. [PubMed: 10565789]
7. (a) Liu Y, Oliveira BL, Correia JDG, Santos IC, Santos I, Spingler B, Alberto R. Org Biomol Chem. 2010; 8:2829. [PubMed: 20445942] (b) Xavier C, Pak JK, Santos I, Alberto R. J Organomet Chem. 2007; 692:1332.(c) Maria L, Paulo A, Santos IC, Santos I, Kurz P, Spingler B, Alberto R. J Am Chem Soc. 2006; 128:14590. [PubMed: 17090043] (d) Mundwiler S, Kuendig M, Ortner K, Alberto R. Dalton Trans. 2004:1320. [PubMed: 15252624] (e) Kurz P, Spingler B, Fox T, Alberto R. Inorg Chem. 2004; 43:3789. [PubMed: 15206855] (f) Kunze S, Zobi F, Kurz P, Spingler B, Alberto R. Angew Chem, Int Ed. 2004; 43:5025.
8. (a) Smith CJ, Sieckman GL, Owen NK, Hayes DL, Mazuru DG, Kannan R, Volkert WA, Hoffman TJ. Cancer Res. 2003; 63:4082. [PubMed: 12874010] (b) Retzloff LB, Heinzke L, Figureoa SD, Sublett SV, Ma L, Sieckman GL, Rold TL, Santos I, Hoffman TJ, Smith CJ. Anticancer Res. 2010; 30:19. [PubMed: 20150613] (c) Lane SR, Veerendra B, Rold TL, Sieckman GL, Hoffman TJ, Jurisson SS, Smith CJ. Nucl Med Biol. 2008; 35:263. [PubMed: 18355681] (d) Alves S, Correia JDG, Gano L, Rold TL, Prasanphanich A, Haubner R, Rupprich M, Alberto R, Decristoforo C, Santos I, Smith CJ. Bioconjugate Chem. 2007; 18:530.(e) Alves S, Correia JDG, Santos I, Veerendra B, Sieckman GL, Hoffman TJ, Rold TL, Figueroa SD, Retzloff L, McCrate J, Prasanphanich A, Smith CJ. Nucl Med Biol. 2006; 33:625. [PubMed: 16843837] (f) Alves S, Paulo A, Correia JDG, Gano L, Smith CJ, Hoffman TJ, Santos I. Bioconjugate Chem. 2005; 16:438.
9. (a) Perera T, Marzilli PA, Fronczek FR, Marzilli LG. Inorg Chem. 2010; 49:2123. [PubMed: 20104873] (b) Perera T, Fronczek FR, Marzilli PA, Marzilli LG. Inorg Chem. 2010; 49:7035. [PubMed: 20593850] (c) Lipowska M, He H, Xu X, Taylor AT, Marzilli PA, Marzilli LG. Inorg Chem. 2010; 49:3141. [PubMed: 20201565] (d) Christoforou AM, Marzilli PA, Fronczek FR, Marzilli LG. Inorg Chem. 2007; 46:11173. [PubMed: 18044880] (e) Christoforou AM, Fronczek FR, Marzilli PA, Marzilli LG. Inorg Chem. 2007; 46:6942. [PubMed: 17655222]
10. (a) Sagnou M, Benaki D, Triantis C, Tsotakos T, Psycharis V, Raptopoulou CP, Pirmettis I, Papadopoulos M, Pelecanou M. Inorg Chem. 2011; 50:1295. [PubMed: 21250638] (b) Sagnou M, Tsoukalas C, Triantis C, Raptopoulou CP, Terzis A, Pirmettis I, Pelecanou M, Papadopoulos M. Inorg Chim Acta. 2010; 363:1649.
11. (a) Chanda N, Shukla R, Zambre A, Mekapothula S, Kulkarni RR, Katti K, Bhattacharyya K, Fent GM, Casteel SW, Boote EJ, Viator JA, Upendran A, Kannan R, Katti KV. Pharm Res. 2011; 28:279. [PubMed: 20872051] (b) Cagnolini A, Ballard B, Engelbrecht HP, Rold TL, Barnes C, Cutler C, Hoffman TJ, Kannan R, Katti K, Jurisson SS. Nucl Med Biol. 2011; 38:63. [PubMed: 21220130] (c) Chanda N, Kattumuri V, Shukla R, Zambre A, Katti K, Upendran A, Kulkarni RR, Kan P, Fent GM, Casteel SW, Smith CJ, Boote E, Robertson JD, Cutler C, Lever JR, Katti K, Kannan R. Proc Natl Acad Sci USA. 2010; 107:8760. [PubMed: 20410458] (d) Chanda N, Shukla R, Katti KV, Kannan R. Nano Lett. 2009; 9:1798. [PubMed: 19351145]
12. (a) Anastasi A, Erspamer V, Bucci M. Experientia. 1971; 27:166–167. [PubMed: 5544731] (b) Erspamer GF, Severini C, Erspamer V, Melchiorri P, Delle Fave G, Nakajima T. Regul Pept. 1988; 21:1–11. [PubMed: 2839869]
13. (a) Qu X, Xiao D, Weber HC. Curr Opin Endocrinol Diabetes. 2003; 10:60.(b) Xiao D, Qu X, Weber HC. Regul Pept. 2002; 109:141. [PubMed: 12409226] (c) Houben H, Denef C. Front Horm Res. 1991; 19:176.
14. (a) Spindel, ER. Handbook of Biologically Active Peptides. Elsevier; New York: 2006. p. 277(b) Flores DG, Lenz G, Roesler R, Schwartsmann G. Cancer Ther. 2009; 7:332.(c) Li X, Lv Y, Yuan A, Li Z. J Cancer Res Clin Oncol. 2010; 136:483. [PubMed: 20140628] (d) Hohla F, Schally AV. Cell Cycle. 2010; 9:1738. [PubMed: 20473035]
15. (a) Bartholdi MF, Wu JM, Pu H, Troncoso P, Eden PA, Feldman RI. Int J Cancer. 1998; 79:82–90. [PubMed: 9495364] (b) Markwalder R, Reubi JC. Cancer Res. 1999; 59:1152–1159. [PubMed: 10070977] (c) Sun BD, Halmos G, Schally AV, Wang XE, Martinez M. Prostate. 2000; 42:295–303. [PubMed: 10679759] (d) Halmos, Wittliff JL.; Schally, AV. Cancer Res. 1995; 55:280–287.

[PubMed: 7812958] (e) Gugger M, Reubi JC. Am J Pathol. 1999; 155:2067–2076. [PubMed: 10595936] (f) Reubi JC, Korner M, Waser B, Mazzucchelli L, Guillou L. Eur J Nucl Med Mol Imaging. 2004; 31:803. [PubMed: 14985869] (g) Reubi JC, Waser B. Eur J Nucl Med Mol Imaging. 2003; 30:781–793. [PubMed: 12707737]

16. (a) Sowrey FE, Blower PJ, Jeffery C, MacLean EJ, Went MJ. Inorg Chem Commun. 2002; 5:832–836.(b) Mullen GED, Blower PJ, Price DJ, Powell AK, Howard MJ, Went MJ. Inorg Chem. 2000; 39:4093–4098. [PubMed: 11198864]

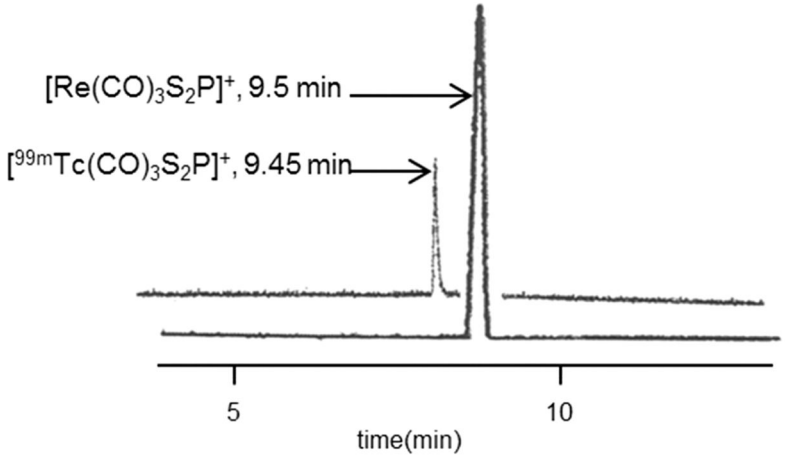

Figure 1.
HPLC chromatograms of $[M(CO)_3(PS_2)]^+$(M = Re (**5**) or ^{99m}Tc (**6**)) complexes.

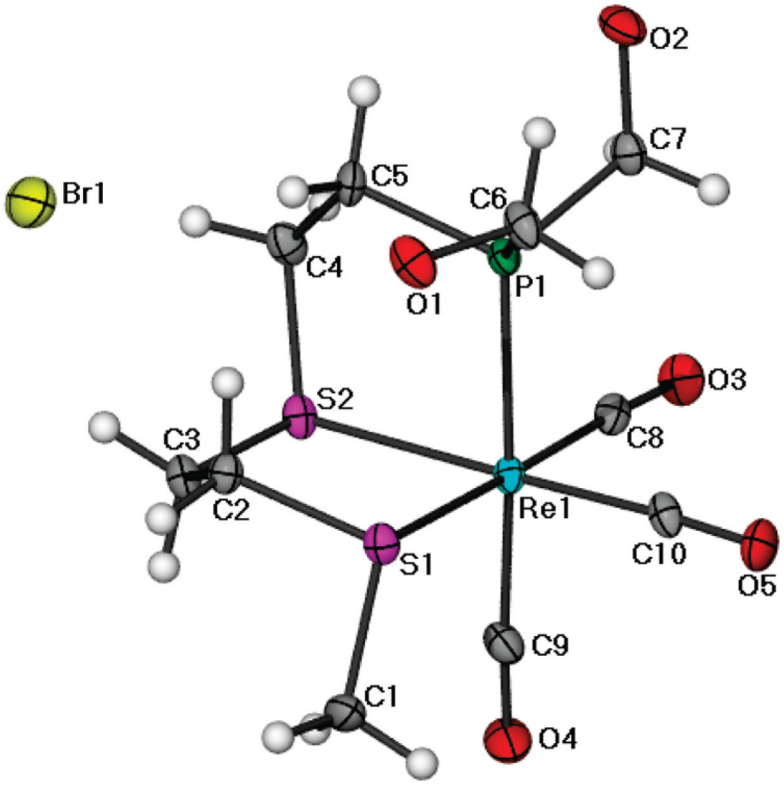

Figure 2.

X-ray crystal structure of **5**. Selected bond lengths (Å) and angles (deg): Re(1)–C(10) = 1.907(10), Re(1)–C(8) = 1.933(10), Re(1)–C(9) = 1.958(11), Re(1)–P(1) = 2.437 (2), Re(1)–S(1) = 2.487(2), Re(1)–S(2) = 2.475(2); P(1)–Re(1)–S(2) = 83.11(8), C(10)–Re(1)–C(8) = 86.9(4), C(10)–Re(1)–C(9) = 91.5(4), C(8)–Re(1)–C(9) = 89.3(4).

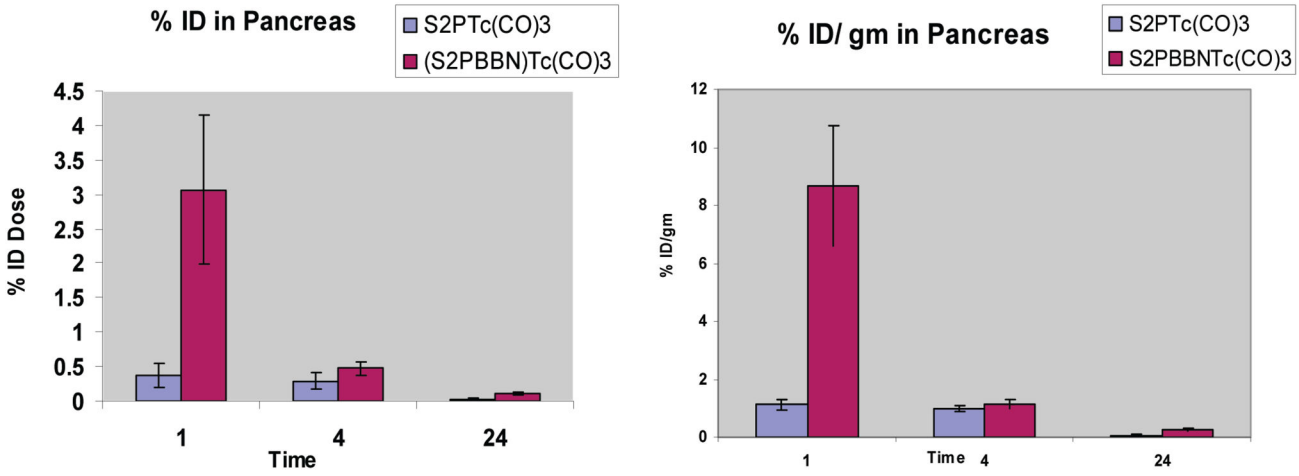

Figure 3.

Comparison of pancreatic uptake between $[^{99m}Tc(CO)_3(PS_2)]_+$ and $[^{99m}Tc(CO)_3(PS_2–BBN)]^+$ in normal CF-1 mice.

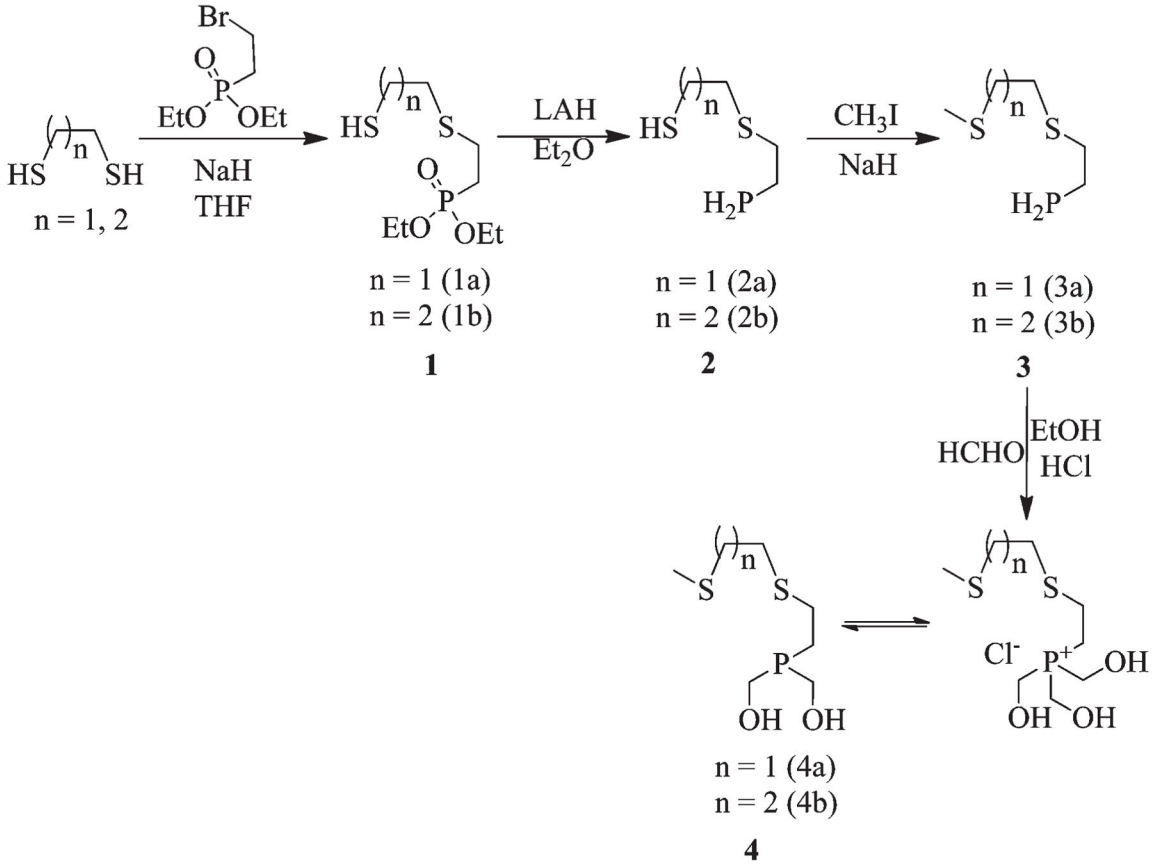

Scheme 1.

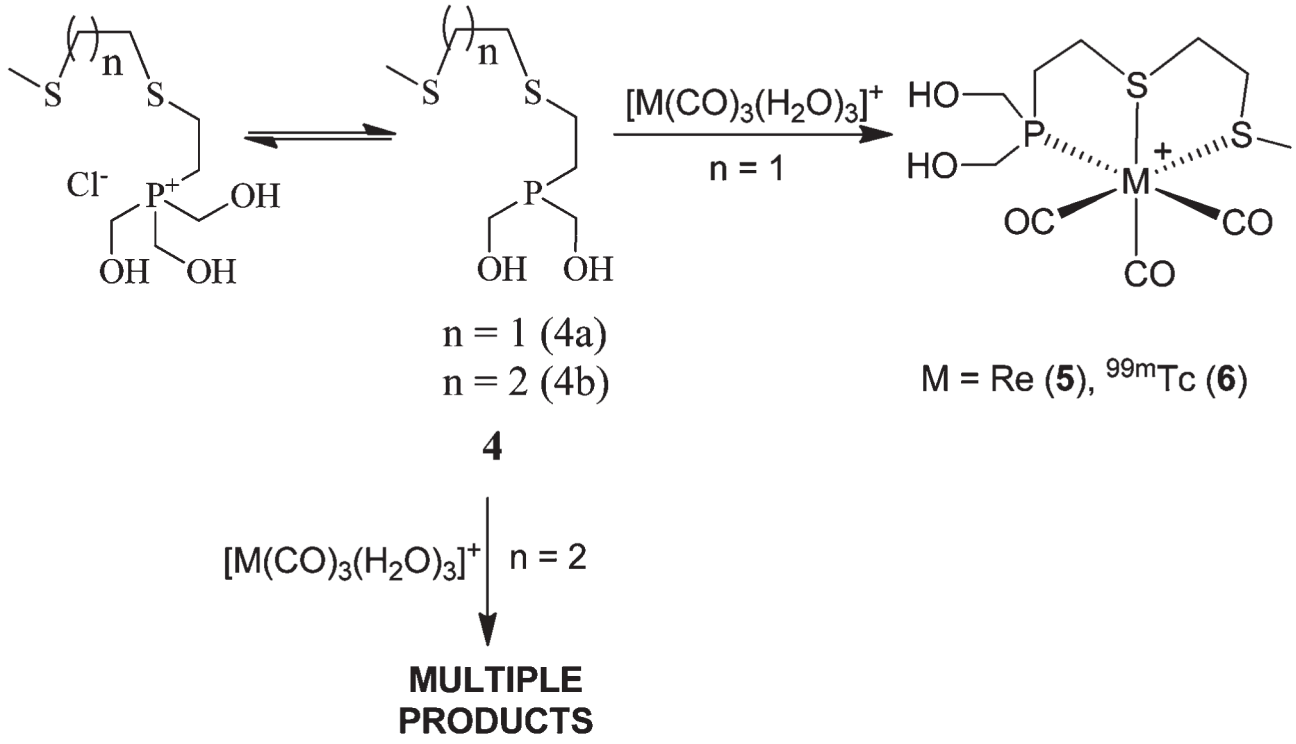

Scheme 2.

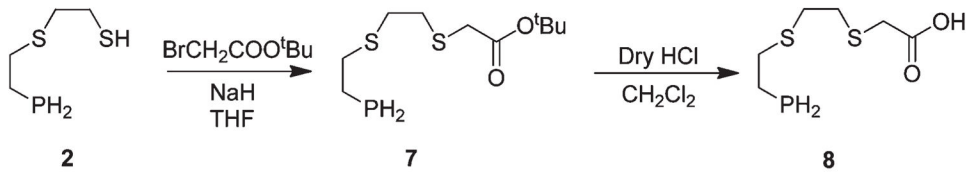

2 **7** **8**

Scheme 3.

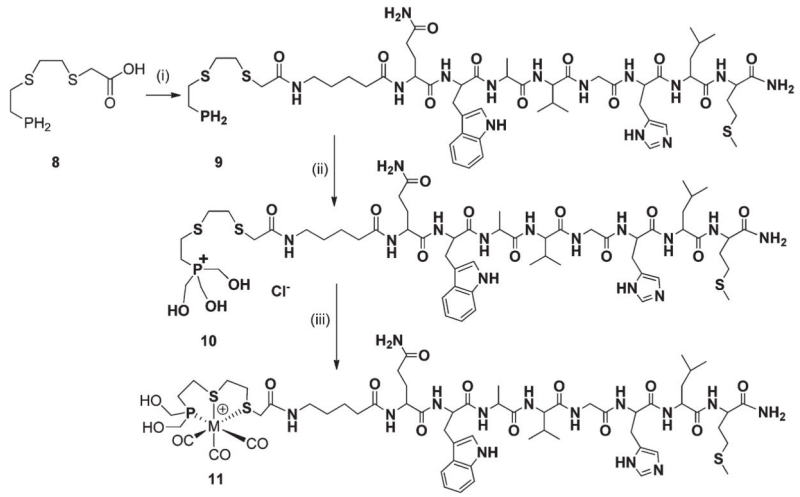

Scheme 4.

Table 1

Crystallographic Data for Complex 5

empirical formula	$C_{10}H_{17}BrO_5PReS_2$
fw	578.44
temp	173(2) K
wavelength	0.71073 Å
cryst syst, space group	triclinic, $P\bar{1}$
unit cell dimensions	a = 6.5967(4) Å, α = 89.0590(10)°, b = 8.9236(5) Å, β = 79.3080(10)°, c = 14.1771(8) Å, γ = 87.8210(10)°
volume	819.43(8) $Å^3$
Z, calcd density	2, 2.344 Mg/m^3
abs coeff	10.217 mm^{-1}
F(000)	548
cryst size	0.45 × 0.15 × 0.15 mm
θ range for data collection	2.28–27.11°
limiting indices	$-8 \le h \le 7$, $-11 \le k \le 11$, $-18 \le l \le 12$
reflns collected/unique	5882/3538 [R(int) = 0.0346]
completeness to θ = 27.11	97.50%
abs correction	semiempirical from equivalents
max and min transm	0.26 and 0.08
refinement method	full-matrix least-squares on F2
data/restraints/params	3538/0/183
GOF on F^2	1.082
final R indices [I > 2σ(I)]	R1 = 0.0549, wR2 = 0.1520
R indices (all data)	R1 = 0.0590, wR2 = 0.1554
extinction coefficient	0.0007(8)
largest diff. peak and hole	3.364 and −4.033 e.A-3

Table 2

Stability of $[^{99m}Tc(CO)_3(PS_2)]^+$ Complex (6) at Different pH's with Time

	percentage (%) of complex remaining		
pH	**1 h**	**4 h**	**24 h**
2	98±1	96±3	94±3
7	98±2	98±1	97± 2
11	97±2	96±2	95±2

Table 3

Biodistribution (% ID/organ[a] and % ID/g[a]) of $[^{99m}Tc(CO)_3S_2P]^+$ (6) in Normal CF-1 Mice 1 h, 4 h, and 24 h, post-IV injection

	time											
	1 h				4 h				4 h			
organ	%ID		%ID/g		%ID		%ID/g		%ID		%ID/g	
brain	0.01	(0.01)	0.03	(0.03)	0.02	(0.02)	0.05	(0.05)	0.01	(0.00)	0.02	(0.01)
blood[b]	0.6	(0.3)	0.22	(0.13)	0.4	(0.1)	0.17	(0.06)	0.00	(0.00)	0.00	(0.00)
heart	0.03	(0.02)	0.20	(0.14)	0.03	(0.01)	0.2	(0.1)	0.03	(0.02)	0.2	(0.1)
lung	0.09	(0.02)	0.40	(0.13)	0.08	(0.03)	0.3	(0.1)	0.04	(0.02)	0.2	(0.1)
liver	6.9	(1.3)	3.8	(0.8)	2.9	(0.9)	1.8	(0.5)	0.6	(0.1)	0.4	(0.1)
spleen	0.08	(0.12)	0.5	(0.7)	0.02	(0.01)	0.17	(0.02)	0.02	(0.02)	0.2	(0.1)
stomach	0.60	(0.21)	1.4	(0.6)	0.4	(0.2)	1.0	(0.6)	0.3	(0.2)	0.4	(0.3)
l. int	16.7	(4.3)	19.1	(11.0)	52.4	(17.1)	58.2	(13.2)	2.7	(2.2)	2.7	(2.1)
sm. int	23.3	(8.7)	13.5	(5.5)	3.1	(1.4)	2.2	(1.4)	0.4	(0.3)	0.3	(0.2)
kidney	1.0	(0.2)	2.2	(0.6)	0.3	(0.1)	0.8	(0.2)	0.10	(0.02)	0.21	(0.04)
urine	46.3	(13.3)			37.4	(18)			68.1	(8)		
muscle	0.02	(0.01)	0.10	(0.06)	0.02	(0.01)	0.12	(0.04)	0.03	(0.02)	0.2	(0.2)
bone	0.01	(0.01)	0.13	(0.06)	0.02	(0.00)	0.2	(0.06)	0.02	(0.02)	0.2	(0.2)
pancreas	0.4	(0.2)	1.1	(0.5)	0.3	(0.1)	1.0	(0.4)	0.02	(0.02)	0.06	(0.07)
carcass	4.5	(1.3)			2.9	(0.6)			1.0	(0.4)		
feces									26	(10)		

[a] Values represent the mean (±SD), *N*= 5 of the% ID/organ or the %ID/g of tissue. Body weights of mice ranged from 21 to 28 g.

[b] Total blood volume is estimated to be 6.5% of the total body weight.

Inorg Chem. Author manuscript; available in PMC 2015 May 15.

Table 4

Biodistribution (%ID/organ[a] and %ID/g[a]) of $[^{99m}Tc(CO)_3S_2P\text{-}BBN]^+$ (11) in Normal CF-1 Mice at 1 h, 4 h, and 24 h, Post-IV-Injection

	time											
	1 h				4 h				24 h			
organ	% ID		%ID/g		% ID		%ID/g		% ID		%ID/g	
tail												
brain	0	(0.00)	0	(0.00)	0	(0.00)	0	(0.00)	0	(0.00)	0	(0.00)
blood[b]	1	(2)	0.67	(0.84)	0.43	(0.12)	0.15	(0.04)	0	(0.00)	0	(0.00)
heart	0.02	(0.01)	0.14	(0.03)	0.01	(0.01)	0.04	(0.02)	0.06	(0.11)	0.4	(0.6)
lung	0.08	(0.06)	0.33	(0.25)	0.03	(0.01)	0.15	(0.04)	0.02	(0.01)	0.07	(0.05)
liver	6.5	(0.8)	3.4	(0.36)	3.3	(0.74)	1.6	(0.4)	0.9	(0.1)	0.4	(0.06)
spleen	0.09	(0.02)	0.66	(0.17)	0.03	(0.01)	0.15	(0.07)	0.02	(0.02)	0.12	(0.17)
stomach	0.52	(0.22)	0.93	(0.42)					0.8	(0.7)	1.1	(0.8)
l. int	16.4	(14)	19.0	(21)	30	(19)	33	(22)	4	(2)	3	(2)
sm. int	42.0	(14)	26.3	(7)	9.3	(6)	5.6	(4.1)	1.1	(0.7)	0.6	(0.4)
kidney	0.49	(0.03)	1.0	(0.1)	0.22	(0.04)	0.44	(0.05)	0.07	(0.01)	0.13	(0.02)
urine	20.3	(6)			45.7	(14)			38	(3)		
muscle	0.03	(0.01)	0.15	(0.04)	0.04	(0.07)	0.2	(0.4)	0.01	(0.02)	0.02	(0.05)
bone	0.01	(0.01)	0.1	(0.06)	0.04	(0.07)	0.5	(1)	0	(0.01)	0.04	(0.08)
pancreas	3.0	(1)	8.7	(2)	0.47	(0.10)	1.1	(0.15)	0.11	(0.02)	0.27	(0.06)
carcass	10.2	(2)			3.7	(1)			1.5	(0.9)		
feces									52.8	(6.6)		

[a] Values represent the mean (±SD), $N = 5$ of the %ID/organ or the %ID/g of tissue. Body weights of mice ranged from 21 to 28 g.

[b] Total blood volume is estimated to be 6.5% of the total body weight.